A THERMAL MODEL FOR OPEN-RACK MOUNTED PHOTOVOLTAIC MODULES BASED ON EMPIRICAL CORRELATIONS FOR NATURAL AND FORCED CONVECTION

Bojan D. PEROVIĆ[1], Dardan O. KLIMENTA[*1], Miroljub D. JEVTIĆ[1], Miloš J. MILOVANOVIĆ[1]

[1]Faculty of Technical Sciences, University of Priština in Kosovska Mitrovica, Kosovska Mitrovica, Serbia

[*]Corresponding author; E-mail: dardan.klimenta@pr.ac.rs

This paper proposes a thermal model for calculating the temperature of open-rack mounted photovoltaic (PV) modules taking into account the meteorological conditions, position (i.e. the inclination of one PV module and the angle between its surface and wind direction) and technical characteristics of the PV modules. The present model is valid for the steady-state operation and is based on the energy balance equation in which the forced convection is modelled by the new empirical correlations. The possibility of occurrence of the flow separation along the surfaces of the PV modules is included in these correlations. The effect of the angle between the wind direction and the PV module plane, which is usually ignored in the modelling of forced convection, is also taken into consideration. In this manner, it is possible to estimate the temperature of PV modules more precisely, as well as to determine the power and efficiency which depend on the temperature. For four particular PV modules, it is found that the temperatures, obtained using the proposed thermal model, are in good agreement with the corresponding measured temperatures. Compared with the other models commonly used for thermal analysis of PV modules (SNL and NOCT-based correlations), this model yielded better results. The deviation of the PV module temperature calculated using the proposed thermal model from the measured one is up to 2 ℃, and the deviations of the PV module temperatures calculated using the SNL and NOCT-based correlations from the measured ones amount up to 5 ℃ and 20 ℃, respectively, depending on the PV module type and ambient conditions.

Key words*: Convection, Flow separation, Modelling, Photovoltaic module, Radiation, Temperature*

1. Introduction

The efficiency of today's commercial PV modules ranges from 13 to 21% [1]. This means, PV modules typically convert more than about 80% of solar radiation reaching their front surfaces into heat. It is also well known that the efficiency of PV modules strongly depends on the physical processes in the structures of PV cells, as well as on environmental conditions [2]. In other words, the efficiency of any PV module decreases significantly with increasing value of its temperature. The major consequence of this strong dependence is a reduction in electricity generation by PV modules. A large number of papers considering the different cooling techniques for PV modules were published. Some of the most commonly used cooling techniques were examined and compared by Grubišić-Čabo *et al.* [3].

Therefore, in order to obtain more accurate estimates of PV modules' temperatures, it is necessary to develop more precise thermal models for PV modules.

As the most commonly used renewable energy generation device, a very large number of publications have so far been dedicated to PV modules. Therefore, a review of papers relating to the estimation of PV modules' temperatures has not been given on this occasion since it would require a lot of space. However, from the literature, it is necessary to single out the NOCT-based (Normal Operating Cell Temperature) and SNL (Sandia National Laboratories) correlations as the most commonly used correlations in thermal modelling of PV modules. According to [2], the NOCT-based correlation for the cell temperature T_{cell} in °C is

$$T_{cell} = T_a + \frac{\mathrm{NOCT} - 20}{800} G \tag{1}$$

where T_a is the air temperature, in [°C], NOCT is the reference value of the cell temperature in [°C], and G is the solar irradiance incident on PV module surface in [W/m^2]. The NOCT is defined as the temperature reached by open circuited cells in a PV module under the following reference conditions [2]: T_a=20 °C, G=800 W/m^2, an average wind velocity v_w=1 m/s, mounting: open-rack, orientation: tilted normally to the solar noon. The correlation (1) is valid only for v_w=1 m/s, which limits its application. According to [4], this correlation may underestimate the cell temperature T_{cell} by up to 20 °C. In addition, the SNL correlation introduces the dependence of the PV module temperature on the wind velocity. This correlation in particular defines the temperature of the back PV module surface [5]

$$T_m = G \times \exp(-3.56 - 0.075 v_w) + T_a \tag{2}$$

in [°C], where G, v_w and T_a are already defined. There are many other models for calculating the temperature of PV modules depending on the various parameters relating to the construction of PV modules or ambient conditions. Some of the most commonly used models are presented in [6, 7], where the models were also compared with each other. The differences in the PV module temperature estimated by individual models were up to 20 °C depending on the wind speed for the same meteorological conditions [6, 7]. Similar differences are also observed when changing the solar irradiance or air temperature [6].

Finally, these large deviations of the calculated PV module temperatures from the actual ones will cause significant changes in the PV module efficiency η_{el}. This means that if there are large differences between these temperatures, the precision and accuracy of the thermal models can not be achieved. This can be best examined by the standard correlation for the PV module efficiency [2]:

$$\eta_{el} = \eta_{T_{ref}} [1 - \beta_{ref} (T_{PV} - T_{ref})] \tag{3}$$

where $\eta_{T_{ref}}$ is the PV module efficiency evaluated at the reference temperature T_{ref} and G=1000 W/m^2, β_{ref} is the efficiency correction coefficient for temperature in [°C^{-1}], and T_{PV} is the PV module operating temperature in [°C]. The values of $\eta_{T_{ref}}$ and β_{ref} are usually given by the manufacturers of PV modules.

This paper proposes a more precise and more accurate thermal model for calculating the temperature of open-rack mounted PV modules based on new empirical correlations for forced convection. The model takes into account the effects of buoyancy forces, wind velocity, angle between the wind direction and the PV module plane, and flow separation along the PV module surfaces. Also, the model is successfully validated with experimental data on four different PV modules reported in the literature.

2. Calculation of the PV module temperature

The calculation of the temperature of an open-rack mounted PV module is based on the following assumptions [8, 9]: (i) The structure consisted of front glass, encapsulant over PV cells, PV cells, encapsulant under PV cells and tedlar backing sheet is assumed to be homogenous, isotropic and isothermal. (ii) The solar absorptivity α_S for the front PV module surface is assumed to be constant and equal 0.97. (iii) The solar absorptivity and thermal emissivity for the front and back PV module surfaces are considered as independent of wavelength. (iv) The four lateral edges of the PV module are considered as adiabatic. (v) The sky is clear. (vi) It is assumed that the PV module operates under steady-state conditions.

This thermal model is based on an energy balance between the energy of solar radiation incident on the front PV module surface $\alpha_S G$, on one side, and the electricity generated in the PV module $\eta_{el}\alpha_S G$ and the heat dissipated by convection and radiation from the PV module surfaces, on the other. This is illustrated in Fig. 1. Accordingly, the energy balance equation for the PV module takes the following form [8, 9]:

$$\alpha_S G = Q_{c,f\to a} + Q_{r,f\to a} + Q_{c,b\to a} + Q_{r,b\to a} + \eta_{el}\alpha_S G \tag{4}$$

where

$$Q_{c,f\to a} = h_f (T_{PV} - T_a) \tag{5}$$

$$Q_{r,f\to a} = h_{r,f} (T_{PV} - T_{sky}) \tag{6}$$

$$h_{r,f} = \varepsilon_f \sigma_{SB}[F_{f\to sky}(T_{PV}^2 + T_{sky}^2)(T_{PV} + T_{sky}) + F_{f\to ground}(T_{PV}^2 + T_g^2)(T_{PV} + T_g)] \tag{7}$$

$$Q_{c,b\to a} = h_b (T_{PV} - T_a) \tag{8}$$

$$Q_{r,b\to a} = h_{r,b} (T_{PV} - T_g) \tag{9}$$

$$h_{r,b} = \varepsilon_b \sigma_{SB}[F_{b\to sky}(T_{PV}^2 + T_{sky}^2)(T_{PV} + T_{sky}) + F_{b\to ground}(T_{PV}^2 + T_g^2)(T_{PV} + T_g)] \tag{10}$$

$$T_{sky} = 0.0552 T_a^{1.5} \tag{11}$$

$$T_g = T_a \tag{12}$$

$$F_{f\to sky} = (1 + \cos\psi)/2 \tag{13}$$

$$F_{f\to ground} = (1 - \cos\psi)/2 \tag{14}$$

$$F_{b\to sky} = [1 + \cos(\pi - \psi)]/2 \tag{15}$$

$$F_{b\to ground} = [1 - \cos(\pi - \psi)]/2 \tag{16}$$

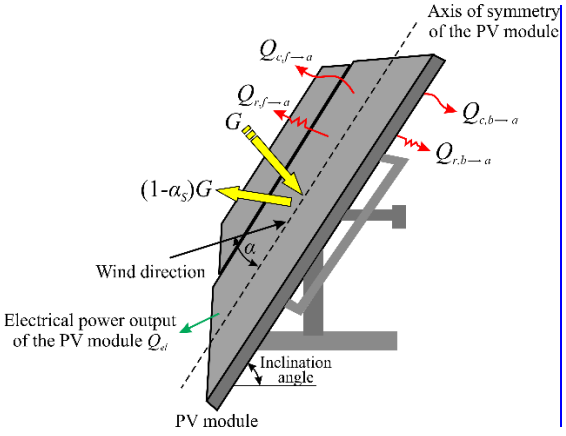

Fig. 1. Illustration of the energy balance equation for the open-rack mounted PV module.

The quantities appearing in equations (4–16) and Fig. 1 have the following meanings: $Q_{c,f\to a}$ and $Q_{c,b\to a}$ are the heat fluxes by natural and/or forced convection between the front and back PV module surfaces and the air in [W/m^2], respectively; $Q_{r,f\to a}$ and $Q_{r,b\to a}$ are the heat fluxes by radiation between the front and back PV module surfaces and the ambient in [W/m^2], respectively; h_f and h_b are the heat transfer coefficients due to mixed (natural and forced) convection between the front and back PV module surfaces and the air in [W·m^{-2}·K^{-1}], respectively; $h_{r,f}$ anf $h_{r,b}$ are the heat transfer coefficients due to radiation between the front and back PV module surfaces and the ambient in [W·m^{-2}·K^{-1}], respectively; $F_{f\to sky}$ and $F_{f\to ground}$ are the view factors between the front PV module surface and the sky, and between the front PV module surface and the ground, respectively; $F_{b\to sky}$ and $F_{b\to ground}$ are the view factors between the back PV module surface and the sky, and between the back PV module surface and the ground, respectively; ε_f and ε_b are the thermal emissivities for the front and back PV module surfaces, respectively; σ_{SB}=5.67·10^{-8} W·m^{-2}·K^{-4} is the Stefan-Boltzmannconstant; T_{sky} and T_g are the sky and ground temperatures in [K], respectively; and α is the angle of incidence of the wind stream on the PV module surface in degrees.

The radiation terms in the equation (4) represent the Stefan-Boltzmann law. The linearisation of the equations relating to the radiation terms is carried out so that the equation (4) also becomes linear. This linearisation is explained in [10]. Bearing this in mind and incorporating equations (5)-(16) into equation (4), the following expression for the PV module temperature is obtained:

$$T_{PV} = \frac{[1-\eta_{T_{ref}}(1+\beta_{ref}T_{ref})]\alpha_S G + (h_f + h_b)T_a + (h_{r,f} + h_{r,b})0.0552\cdot T_a^{1.5}}{h_f + h_{r,f} + h_b + h_{r,b} - \eta_{T_{ref}}\beta_{ref}\alpha_S G} \qquad (17)$$

After determining the value of T_{PV}, the values of $(T_{PV}^2 + T_{sky}^2)(T_{PV} + T_{sky})$ and $(T_{PV}^2 + T_g^2)(T_{PV} + T_g)$ are recalculated using equations (7) and (10), and a new value for T_{PV} is generated. An almost exact solution is obtained after several iterations.

The values for h_f and h_b are estimated using the correlations for natural and forced convection between the front and back PV module surfaces and the air. The correlations for natural convection are given in [9], while the correlations for forced convection are derived in the next section. The correlations for natural convection from [9] include the effects of the inclination angle and flow separation. The proposed thermal model is more complicated than the SNL and NOCT-based correlations because it incorporates the more complex and more precise correlations for natural and forced convection. In addition, as opposed to the SNL and NOCT-based correlations, the proposed thermal model considers the effects of the optical and physical properties of the PV module, and takes into account the effect of the PV module position (i.e. the effect of the inclination angle).

3. Correlations for forced convection

There are many different correlations for calculating the heat transfer coefficient due to forced convection between the front and back PV module surfaces and the air, either directly or by means of the Nusselt number [11]. The differences between the PV module temperatures obtained using different correlations for the same environmental conditions can reach several tens of percentage points [6]. On the other hand, there are a few correlations which take into account the angle between the wind direction and the PV module surface, that is, the angle α (Fig. 1). The effect of this angle is small, but it cannot be ignored in a precise analysis of the PV module performance [12].It is evident from the experimental data collected from the literature and used in [12] that the heat transfer coefficient due to forced

convection for the windward side of a PV module hwindward decreases with increasing the angle α in the whole range of values from 0° to 90°. This decrease is small and linear up to the value of the angle α of approximately 40°. For α=40°, the value of hwindward suddenly decreases by a few percentage points. Any further increase in the angle α above 40° causes a very low decrease in the coefficient hwindward. This is the phenomenon known in the scientific literature, and it is due to the formation of a separation bubble on the leading edge of a PV module for α<40°. The flow becomes turbulent after reattachment and hence the heat transfer coefficient due to forced convection is higher. According to [13], the critical angle below which there could be a separation bubble is about 40°. In case of higher angles, there is no separation and the flow remains laminar along the PV module. This is valid for the values of the Reynolds number Re≤5·105 for which the flow is considered to be laminar [14]. For the values of the Reynolds number Re>5·105, regardless of the angle α and other flow conditions, it is assumed that the flow is turbulent [9,14].Based on the correlation proposed by Kendoush [15] and the experimental results used in [12], the dependence of the coefficient $h_{windward}$ on the angle α, wind velocity v_w, and characteristic length L_c can be expressed as follows:

$$h_{windward} = a_1 \Phi^{b_1} L_c^{c_1} (\cos\alpha)^{d_1} \text{ for } \alpha<40°, \text{ and} \tag{18}$$

$$h_{windward} = a_2 \Phi^{b_2} L_c^{c_2} (\sin\alpha)^{d_2} \text{ for } \alpha\geq 40°, \tag{19}$$

where

$$\Phi = \frac{\mathrm{Re}\,\mathrm{Pr}^{2/3}}{[1+(0.0468/\mathrm{Pr})^{2/3}]^{1/2}} \tag{20}$$

is the Churchill's dimensionless parameter for forced convection from flat plates [16], and

$$\mathrm{Re} = \frac{\rho v_w L_c}{\mu} \tag{21}$$

After defining the parameter Φ, it is possible to calculate the coefficient $h_{windward}$ for any value of the Reynolds number. According to the available literature, the correlations (18) and (19) are the only correlations for determining the heat transfer coefficient due to forced convection which take into account the variables α, $v_w$and L_c, and which are valid in a wide range of Reynolds and Prandtl numbers. The correlation coefficients a_1, b_1, c_1, d_1, a_2, b_2, c_2 and $d_2$are unknown and will be determined under the condition that the correlations (18) and (19) represent the best approximation for the experimentally obtained values of the coefficient $h_{windward}$. The genetic algorithm (GA) and the least squares method are used to determine the aforementioned coefficients.

A general optimisation problem can be described as follows [17]:

$$\min F(\mathbf{x},\mathbf{u}) \tag{22}$$

$$\mathbf{g}(\mathbf{x},\mathbf{u}) = 0 \tag{23}$$

$$\mathbf{e}(\mathbf{x},\mathbf{u}) \leq 0 \tag{24}$$

where $F(\mathbf{x},\mathbf{u})$ is an objective function,$\mathbf{x}$ is a vector of design variables, $\mathbf{u}$ is a vector of control variables, $\mathbf{g}(\mathbf{x},\mathbf{u})$ is a vector composed of equality constraints and $\mathbf{e}(\mathbf{x},\mathbf{u})$ is a vector composed of inequality constraints.The optimisation process is carried out twice: once for α<40° in order to determine the coefficients a_1, b_1, c_1, and d_1, and once for $\alpha\geq$40° in order to determine the coefficients a_2, b_2, c_2, and d_2. The vector of control variables $\mathbf{u}$, whose values will be optimised using the GA, is defined as:

$$\mathbf{u} = [a_1, b_1, c_1, d_1]^{\mathrm{T}} \text{ for } \alpha<40°, \text{ and} \tag{25}$$

$$\mathbf{u} = [a_2, b_2, c_2, d_2]^{\mathrm{T}} \text{ for } \alpha \geq 40°. \tag{26}$$

In both cases, the objective function represents the sum of the squares of the differences between the calculated $h_{windward}$ and experimentally determined $h_{windward,i}$ values, i.e.

$$F = \sum_i [a_1 \Phi_i^{b_1} L_{ci}^{c_1} (\cos\alpha_i)^{d_1} - h_{windward,i}]^2 \text{ for } \alpha < 40°, \text{ and} \tag{27}$$

$$F = \sum_i [a_2 \Phi_i^{b_2} L_{ci}^{c_2} (\cos\alpha_i)^{d_2} - h_{windward,i}]^2 \text{ for } \alpha \geq 40°, \tag{28}$$

where the values of $h_{windward}$ are calculated using correlation (18) and (19), respectively.
The values for $h_{windward,i}$ in function of v_w, for given values of α, are obtained from the dependences of the Nusselt number Nu [18,19], Stanton number St [20] and Colburn factor [21,22] on the Reynolds number for different values of α, v_w and L_c, or from the dependence of heat losses from a flat-plate collector on v_w [23].This was accomplished by simple mathematical operations. Then all values of the coefficient $h_{windward,i}$ are adapted to a characteristic length L_c that equals four times the area $4A$ (of one side) of a flat plate divided by its perimeter P (i.e. $L_c=4A/P$).

Using the values of a_1, b_1, c_1, d_1, a_2, b_2, c_2 and d_2 obtained by means of the GA, the correlations for the heat transfer coefficient due to forced convection from the windward side of the PV module can be expressed as follows:

$$h_{windward} = 0.01 \Phi^{0.61} L_c^{-1} (\cos\alpha)^{0.72} \text{ for } \alpha < 40°, \text{ and} \tag{29}$$

$$h_{windward} = 0.023 \cdot \Phi^{0.5} \cdot L_c^{-1} \cdot (\sin\alpha)^{-0.234} \text{ for } \alpha \geq 40°. \tag{30}$$

Comparisons between the correlations (29) and (30) and corresponding experimental data are presented in Fig. 2. Most of experimental data used here are valid for $\mathrm{Re} \leq 2 \cdot 10^5$. This means that the correlations (29) and (30) are also valid for the same range of Reynolds numbers.

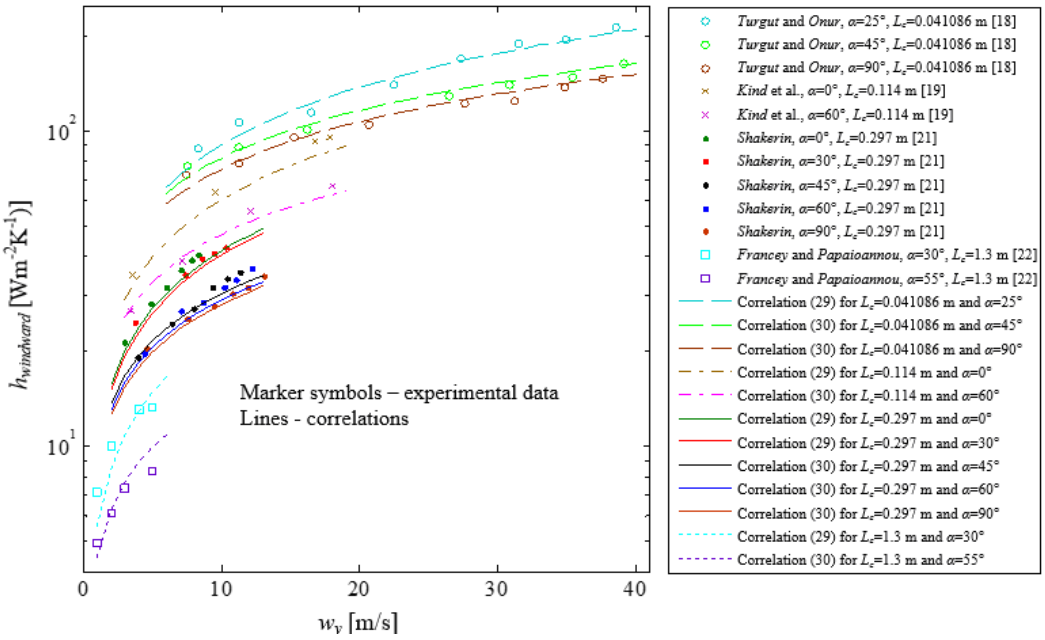

Fig. 2. Comparisons of correlations (29) and (30) with heat transfer coefficients due to forced convection calculated fromthe existing experimental data.

The correlations (29) and (30) are derived for a ratio of the plate length L to its width W, which is less than or equal to 3. It is therefore obvious that the ratio $L/W \leq 3$ can be introduced as a limiting

criterion for these two correlations, although, according to [24], this ratio does not affect the coefficient $h_{windward}$.The particular question that arises here is this: which correlations can be used to determine the coefficient $h_{windward}$ for Reynolds numbers larger than $2\cdot10^5$?

A correlation for heat transfer due to turbulent forced convection between the PV module and the surrounding air is proposed in the following form [10]:

$$\mathrm{St}\,\mathrm{Pr}^{0.4} = 0.028\,\mathrm{Re}^{-0.2} \tag{31}$$

which is valid for $\mathrm{Re}>1.2\times10^5$. In order to express the heat transfer due to turbulent forced convection in terms of the coefficient $h_{windward}$ instead of the Stanton number St, some algebraic manipulations should be performed. After these manipulations, the correlation (31) becomes:

$$h_{windward} = 0.029 k_t \Phi^{0.8} L_c^{-1} \tag{32}$$

The effect of the angle α is not included in the correlations (31) and (32). According to [25], this effect is negligible for flat plates having large dimensions (i.e. characteristic lengths). This is also in agreement with the observation of a noticeable effect of the angle α on the correlations (29) and (30) for larger characteristic lengths. The correlations (29) and (30) are relevant for $\mathrm{Re}\le2\cdot10^5$, while the correlation (32) is valid for $\mathrm{Re}>1.2\times10^5$. Consequently, there is an overlapping between the laminar and turbulent flow regimes. In order to separate these flow regimes, the following critical Reynolds numbers are defined:

$$\mathrm{Re}_{cr,\,\alpha<40^o} = \frac{\left(\dfrac{0.029k_t}{0.01(\cos\alpha)^{0.72}}\right)^{-1/0.19}}{\dfrac{\mathrm{Pr}^{2/3}}{[1+(0.0468/\mathrm{Pr})^{2/3}]^{1/2}}} \tag{33}$$

for the correlations (29) and (32), and

$$\mathrm{Re}_{cr,\,\alpha\ge40^o} = \frac{\left(\dfrac{0.029k_t}{0.023(\sin\alpha)^{-0.234}}\right)^{-1/0.3}}{\dfrac{\mathrm{Pr}^{2/3}}{[1+(0.0468/\mathrm{Pr})^{2/3}]^{1/2}}} \tag{34}$$

for the correlations (30) and (32). Determination of the $\mathrm{Re}_{cr,\alpha<40^\circ}$ and $\mathrm{Re}_{cr,\alpha\ge40^\circ}$ values was carried out by equalising the corresponding pairs of overlapping correlations.

The correlations (29), (30) and (32) are derived under the assumption that there is no obstacle to the wind direction towards the front PV module surface. However, if the wind flows towards the back surface of the PV module mounted on the ground, the wind can encounter obstacles such as the frame/base and mechanism for single-axis or dual-axis solar tracking system (if any). This is the case where the back PV module surface can be treated as a windward surface. In this case only, when the wind velocity is greater than 3 $\mathrm{m\cdot s^{-1}}$, the flow regime will be considered as turbulent. Regardless of the value of the Reynolds number, and based on the research conducted by Sartori [26], the following correlation for heat transfer coefficient due to forced convection:

$$h_{windward} = \frac{0.037\,\mathrm{Re}^{4/5}\,\mathrm{Pr}^{1/3}\,k_t}{L_c} \tag{35}$$

was introduced and standardised by Kaplani and Kaplanis [8]. In this correlation, k_t represents the thermal conductivity in $[\mathrm{W\cdot m^{-1}\cdot K^{-1}}]$, and the Reynolds number should be determined.

When the wind velocity is lower than 3 m/s, it is necessary to calculate the value of the Reynolds number. If $\alpha<40°$ and $Re<Re_{cr,\alpha<40°}$ then the correlation (29) should be applied, and if $\alpha\geq40°$ and $Re\leq Re_{cr,\alpha\geq40°}$ then the correlation (30) should be used. Otherwise, for any value of the angle α, the correlation (32) should be applied.For forced convection from the leeward side of the PV module and any direction of the wind, the following correlations can be used [8]:

$$h_{leeward} = 3.83 v_w^{0.5} L_c^{-0.5} \text{ for laminar flow} \tag{36}$$

$$h_{leeward} = 5.74 v_w^{0.8} L_c^{-0.2} - 16.46 L_c^{-0.2} \text{ for transitional flow, and} \tag{37}$$

$$h_{leeward} = 5.74 v_w^{0.8} L_c^{-0.2} \text{ for fully developed turbulent flow.} \tag{38}$$

The correlations (36 – 38) were proposed by Sartori[26], and were originally applied when the length of the PV module in the direction of the wind was used as the characteristic length L_c. However, Kaplani and Kaplanis[8] found that these correlations give more accurate results when the characteristic length L_c equals

$$L_c = 4A / P \tag{39}$$

where A is the area of one side of the PV module, and P is the perimeter of the PV module. The characteristic length (39) is used here for the correlations (36 – 38).

In order to determine whether the wind flow regime is laminar, transitional or turbulent, a ratio of the critical length x_c to the characteristic length L_c is required for selecting the correlation for the coefficient $h_{leeward}$. In addition, the critical length x_c is given by:

$$x_c = \frac{\mathrm{Re}_{cr}\, \nu}{v_w} \tag{40}$$

where ν is the kinematic viscosity of the air in [m^2/s], and $Re_{cr}$is the critical Reynolds number that, in accordance with [8, 25], equals $4\cdot10^5$. According to the value of the x_c/L_c ratio, there are three manners to select the correlation for the coefficient $h_{leeward}$, as follows: (i) if $x_c/L_c\geq0.95$ then correlation (36) should be applied, (ii) if $0.05<x_c/L_c<0.95$ then correlation (37) should be applied, and (iii) if $xc/L_c\leq0.05$ then correlation (38) should be applied.

4. Mixed convection

The three types of heat transfer by convection are usually categorised according to the ratio $Gr_L/(Re_L)^2$, where

$$\mathrm{Gr}_L = \frac{\rho^2 \beta g (T_{PV} - T_a) L^3}{\mu^2} \tag{41}$$

is the Grashof number defined in terms of the characteristic length L, L is the length of the PV module in the direction of the buoyancy force in [m], ρ is the air density in [kg/m^3], β is the thermal expansion coefficient of the air in [1/K], g is the acceleration due to gravity in [m/s^2], T_{PV} is the PV module temperature in [K], T_a is the air temperature in [K], and μ is the dynamic fluid viscosity in [m^2/s^1]. In addition, Re_L is the Reynolds number based on the characteristic length L_c given by equation (21). If $Gr_L/(Re_L)^2\leq0.01$ or $Gr_L/(Re_L)^2\geq100$, the effect of natural or forced convection is negligible, respectively. Also, natural convection dominates when $Gr_L/(Re_L)^2\geq100$. If $0.01<Gr_L/(Re_L)^2<100$, both effects are significant and must be considered.

The heat transfer coefficients due to mixed convection between the front and back PV module surfaces and the airh_f and h_b can be calculated using these correlations [27]:

$$h_f^3 = h_{f(\,forced\,)}^3 + h_{f(natural)}^3 \tag{42}$$

$$h_b^3 = h_{b(\,forced\,)}^3 \pm h_{b(natural)}^3 \tag{43}$$

Forced flow assisting or opposing the motion generated by the natural convection around the PV module is taken into account. For the front PV module surface, the forced flow is assisting to the buoyancy-driven motion, whereby only the positive sign is used in the equation (42). For the back PV module surface, the assisting forced flow is considered if this surface is leeward, whereby the positive sign is used in the equation (43); and the opposing forced flow if this surface is windward, whereby the negative sign is used [8].Fig. 3 shows the flowchart of the proposed thermal model for calculation of the PV module temperature T_{PV}. According to Fig. 3, L_{PV} and W_{PV} are the length and width of a PV module, respectively. All the other parameters included in this flowchart are already defined.

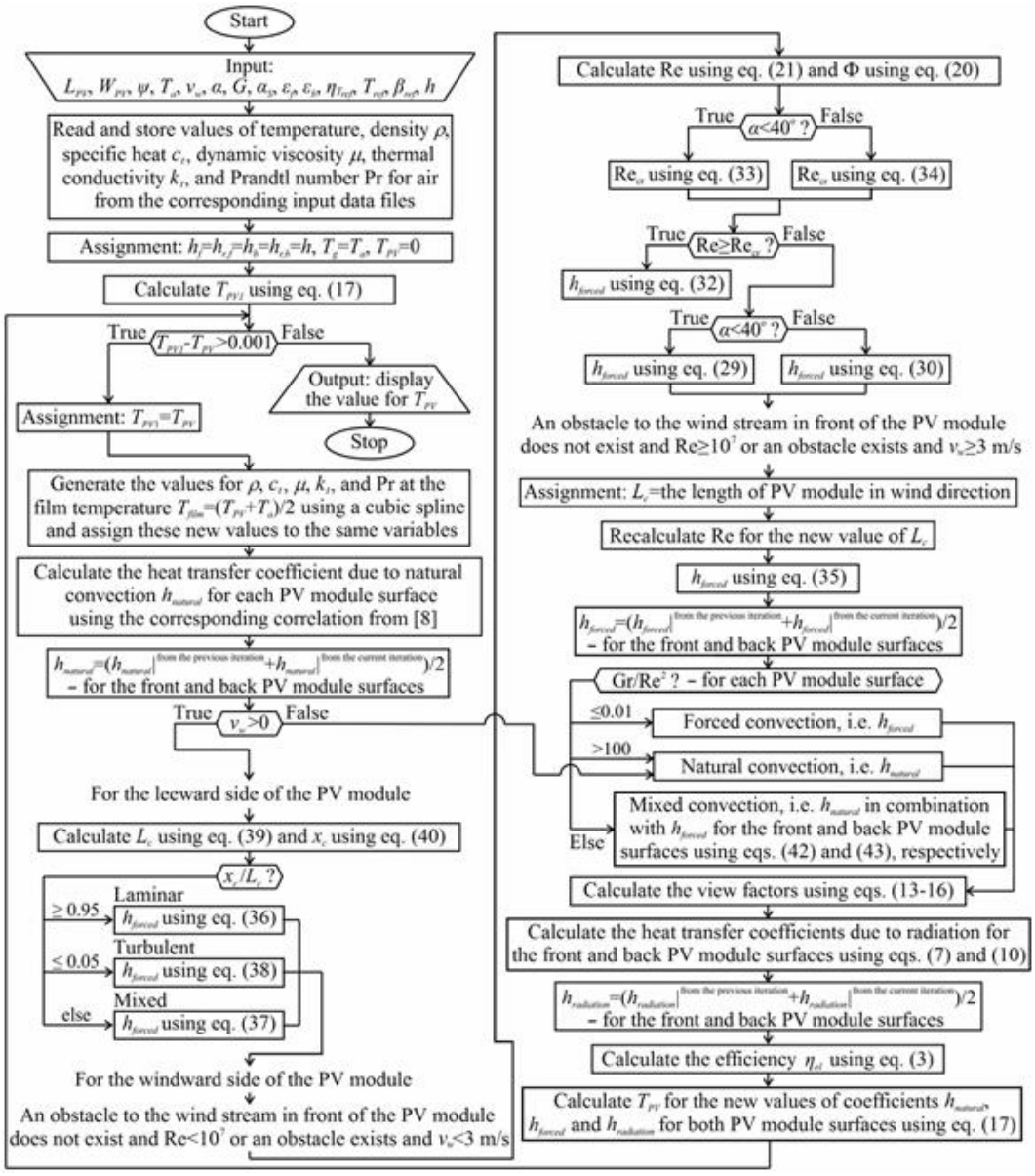

Fig. 3. Flowchart of the proposed thermal model.

5. Results and discussion

In order to confirm the accuracy of the developed thermal model, the experimental results obtained by Nižetić*et al.* [28] for the poly-crystalline and mono-crystalline PV modules were used. The poly-crystalline PV module dimensions were 0.65 m×0.6 m, while the mono-crystalline dimensions were 0.55 m×0.65 m. The efficiencies of the poly-crystalline and mono-crystalline PV modules were 0.132 and 0.144, respectively. Fig. 4 shows the temperatures of the poly-crystalline PV module of the type SL-50P obtained using the proposed model, NOCT-based correlation (1) and SNL correlation (2) in comparison to the corresponding temperatures measured by thermocouples during a period of 180 s [28]. The corresponding mean measured temperature is also presented in Fig. 4.

According to Fig. 4, the four curves represented by marker symbols refer to the temperatures measured at the four different points on the back PV module surface, while the dashed line relates to the mean of these temperatures over the 180-second period. The measurements were performed using thermocouples installed directly on the siliceous cells (the polyvinyl fluoride layer of the PV module was purposely drilled).

The measured and calculated temperatures for the poly-crystalline PV module are determined under the same environmental conditions, namely [28]: G=906 W/m^2, T_a=21 °C, v_w=1 m/s^1, β=20°, α=20°, NOCT=48 °C, and the front PV module surface is windward.

The temperature of the mono-crystalline PV module of the type SL-50AA36 was experimentally determined by Nižetić *et al.* [28] for several different values of the wind velocity v_w, solar irradiance G and angle α. In [28], the temperature of this mono-crystalline PV module was also calculated by means of ANSYS Fluent CFD software for the same environmental conditions. Tab. 1 compares the mean values of these measured and simulated temperatures with the corresponding temperatures obtained using the proposed thermal model, NOCT-based correlation (1) and SNL correlation (2).

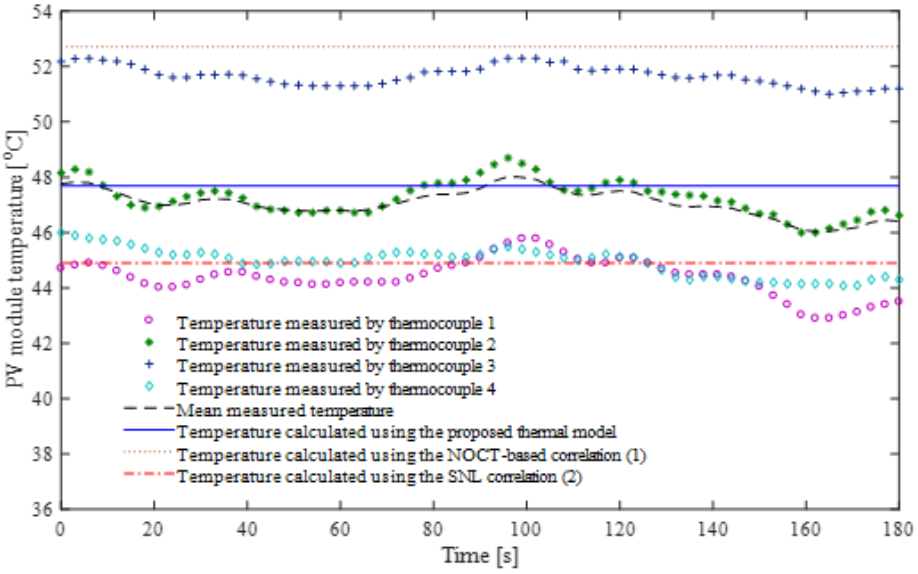

Fig 4. Comparison between measured and calculated temperatures of the poly-crystalline PV module of the type SL-50P when it is inclined at an angle of 20° to the horizontal.

From Fig. 4 and Tab. 1, it can be seen that the NOCT-based correlation (1) overestimates the PV module temperature and that the SNL correlation (2) generally gives lower values for this

temperature. Compared to the temperatures calculated using the NOCT-based and SNL correlations, the temperatures obtained by means of the proposed thermal model are in better agreement with the measured ones.

In order to continue comparing the PV module temperatures obtained using the proposed model with those measured for different values of the air temperature T_a, wind velocity v_w and solar irradiance G, the experimental results reported in [29] are used. Kouadri Boudjelthia *et al.* [29] performed experiments with a south-facing mono-crystalline PV module inclined at the angle of 37° (with respect to horizontal) that represents the optimal inclination angle for PV modules in the city of Algiers. For the purpose of temperature measurements, three thermocouples were installed on the back PV module surface (on the polyvinyl fluoride layer). The efficiency and dimensions of this PV module were 0.142 and 1.1938 m×0.55 m, respectively. The corresponding comparison between measured and calculated PV module temperatures for different values of T_a, v_w and G is shown in Fig. 5.

Tab. 1. Comparison between measured and calculated temperatures of the mono-crystalline PV module of the type SL-50AA36 when it is inclined at an angle of 20° to the horizontal.

Conditions	Method, model or correlation	Temperature at measurement points*				Mean temperature [°C]
		Point 1 [°C]	Point 2 [°C]	Point 3 [°C]	Point 4 [°C]	
Case 1: v_w=1.5 m·s^{-1}, α=45°, G=837 W·m^{-2}, T_a=28.3 °C, NOCT=48 °C, inclination of PV module is 45°	Experimental, [28]	47.84	49.84	51.84	56.84	51.59
	CFD, [28]	46.84	46.84	47.84	46.84	47.09
	Proposed model	–	–	–	–	52.23
	NOCT-based	–	–	–	–	57.59
	SNL	–	–	–	–	49.57
Case 2: v_w=2.7 m·s^{-1}, α=0°, G=837 W·m^{-2}, T_a=28.3 °C, NOCT=48 °C, inclination of PV module is 0°	Experimental, [28]	40.84	43.84	44.84	48.84	44.59
	CFD, [28]	41.84	42.84	44.84	42.84	43.09
	Proposed model	–	–	–	–	46.58
	NOCT-based	–	–	–	–	57.59
	SNL	–	–	–	–	47.74

* Points at which thermocouples were installed directly on the siliceous cells.

Based on Fig. 5, it is evident that the values of the PV module temperature obtained by the proposed thermal model and SNL correlation (2) agree quite well with the results of measurements performed by Kouadri Boudjelthia *et al.* [29]. However, the NOCT-based correlation (1) significantly overestimates the experimental results. This is expected because the NOCT-based correlation is valid for v_w=1 m/s, which is considerably lower than the values of v_w corresponding to the measured values of the PV module temperature. Over most of the observed period, the PV module temperature calculated using the proposed model is higher by about 2 °C than the measured one. It should be noted here that the measured temperature of the PV module refers to its back surface and that the actual cell temperature inside the PV module is higher by about 1-2 °C [8]. Therefore, the PV module temperature calculated using the proposed model is well-matched to the measured one.

In addition, the measured response of the PV module temperature to changes in environmental conditions is not as sharp as the one calculated using the proposed model or SNL correlation. This is due to the fact that the thermal capacities of PV module materials were neglected in the proposed model, as well as in the SNL correlation. For the same reason, the values of the PV module temperature obtained using the proposed model and SNL correlation are lower than the measured ones in the period from about 16:00 to 17:40 (Fig. 5). In particular, since the PV module was exposed to significantly higher solar irradiance before 16:00, there were no sufficient cooling mechanisms to dissipate accumulated heat to the environment during the period from 09:25 to about 16:00.

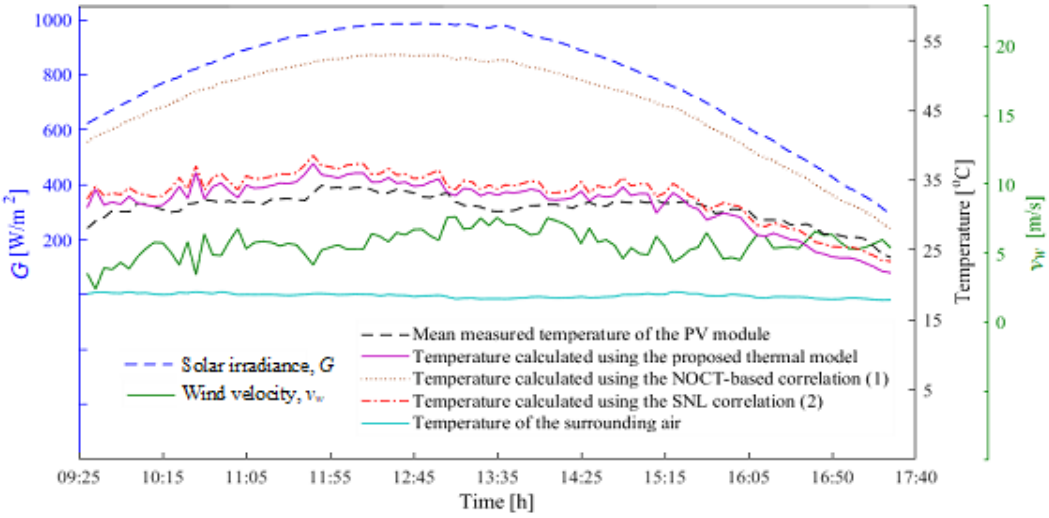

Fig 5. Comparison between measured and calculated temperatures of the mono-crystalline PV module when it is inclined at an angle of 37° to the horizontal for different values of T_a, v_w and G [29].

All previous results were related to wind velocities different from 0 m/s. In order to validate the proposed model with data on wind velocities very close to or equal to zero, the present work will be compared and contrasted with the experimental work of Palacio Vega*et al.* [30]. According to [30], the experiments were carried out in Córdoba, Colombia, from 10:00 to 14:00. The experimental apparatus was consisted of a Winbright YB125M72-200W PV module positioned horizontally and exposed to the typical environmental conditions. The efficiency and dimensions of this PV module were 0.1778 and 1.58 m×0.808 m, respectively. Fig. 6 compares the PV module temperatures obtained using the proposed thermal model, NOCT-based correlation (1) and SNL correlation (2) with the corresponding measured values taken from [30]. This comparison is performed for the 15th day of April in the year 2016, because fluctuations in solar irradiance were small on that day between 11:00 and 12:25. Accordingly, during the considered period, there were no large fluctuations in the PV module temperature, i.e. the PV module operated in a near-steady-state regime for which the proposed model is valid.

From Fig. 6, it can be seen that over the period from 11:00 to about 12:25, the PV module temperatures calculated using the proposed model, on average, are about 2 °C higher than the measured ones. It is also evident from Fig. 6 that over the period under consideration, these temperatures agree well with each other. In addition to this, the temperatures calculated using the NOCT-based correlation (1) are lower by about 1 °C than the temperatures obtained using the proposed model; and the

temperatures calculated using the SNL correlation (2) are lower by about 5 °C than the measured ones (which refer to the temperature of the back PV module surface). Moreover, there were large fluctuations in solar irradiance between about 12:25 and 14:00. The temperature curves obtained by means of the proposed model, NOCT-based correlation and SNL correlation follow these fluctuations, but the same cannot be said for the curve of the mean measured temperature. This is caused by ignoring the thermal capacities of PV module materials in the calculations, i.e. the proposed model, as well as the SNL and NOCT-based correlations, solves steady-state problems (not dynamic ones). Furthermore, the temperature data acquisition was repeated every 15 minutes until 14:00, which represents a long time interval from the aspect of the rate of solar irradiance change. Therefore, for the period from about 12:25 to 14:00, it was not realistic to expect any concordance between measured and calculated temperatures of the PV module.

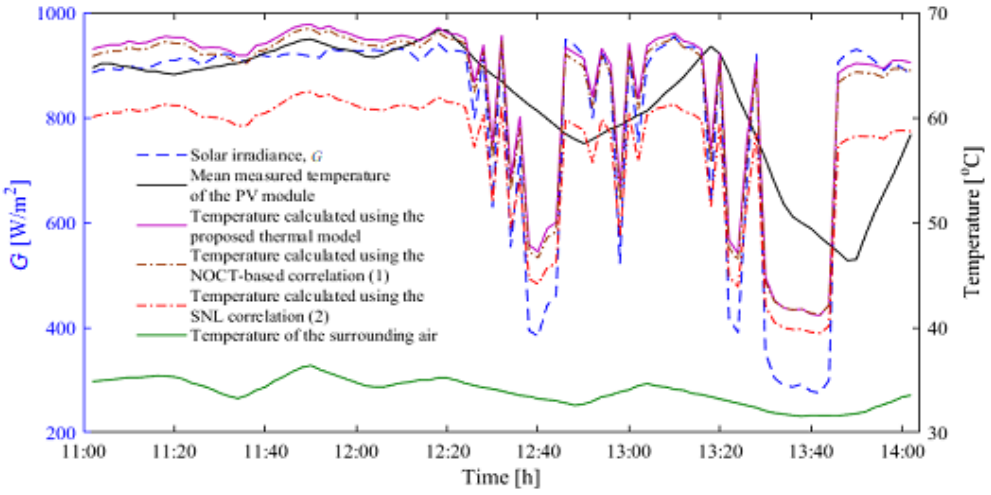

Fig 6. Comparison between measured and calculated temperatures of the mono-crystalline PV module which is positioned horizontally and analysed in [30] for different values of T_a and G.

In all these cases, with the exception of the Winbright YB125M72-200W PV module for which β_{ref} was equal to 0.0047, the calculations of the PV module temperature were performed with the following parameters: α_S=0.97, ε_f=0.85, ε_b=0.91, β_{ref}=0.0041 and T_{ref}=298.157 K.

6. Conclusion

The overall conclusions that can be drawn from the presented results and discussion are as follows:

- The proposed thermal model for calculating the temperature of open-rack mounted PV modules is new, it could be used in a wider range of applications (i.e. in a wider range of Reynolds and Prandtl numbers) and it can be easily integrated into commercial software packages.
- With respect to the NOCT-based and SNL correlations, the proposed thermal model appears to be considerably more complex, but more detailed, precise and accurate.
- The new empirical correlations for forced convection from the flat-plate PV modules at various environmental and operating conditions are in excellent agreement with the existing correlations and experimental data.

- Since the proposed thermal model allows a more precise calculation of the PV module temperature, it means that the temperature-dependent performance characteristics of the PV modules (output power and efficiency) can also be properly assessed.
- The proposed thermal model includes the effects of buoyancy forces, flow separation, inclination angle, angle between the wind direction and the PV module plane, and so on, which makes it unique compared to other models for determining temperatures and optimal inclinations for fixed flat-plate PV modules and panels.

In addition to these conclusions, it is planned to develop a dynamic thermal model that will take into account the thermal capacities of PV module materials, as well as large fluctuations in solar irradiance over shorter periods of time.

Acknowledgements: This paper was based on research conducted within the project TR33046.

7. References

[1] World Energy Resources 2016 – Solar, World Energy Council, London, UK, 2016, https://www.worldenergy.org/publications/2016/world-energy-resources-2016/
[2] Skoplaki, E., *et al.*, A simple correlation for the operating temperature of photovoltaic modules of arbitrary mounting,*Solar Energy Materials and Solar Cells*, 92(2008), 11, pp. 1393-1402
[3] Grubišić-Čabo, F*et al.*, Photovoltaic Panels: A Review of the Cooling Techniques, *Transactions of FAMENA*, 40(2016), SI-1, pp. 63-74
[4] Davis, M. W., *et al.*, Prediction of building integrated photovoltaic cell temperatures,*Journal of Solar Energy Engineering*, 123(2001), 3, pp. 200-210
[5] King, D. L., *et al.*, Photovoltaic array performance model, Sandia Report SAND2004-3535, Unlimited Release, Sandia National Laboratories, USA, 2004
[6] Jakhrani, A. Q., *et al.*, Comparison of solar photovoltaic module temperature models, *World Applied Sciences Journal*, 14(2011), pp. 1-8
[7] Denoix, T., *et al.*, Experimental comparison of photovoltaic panel operating cell temperature models, Proceedings of the IECON 2014 – 40th Annual Conference of the IEEE Industrial Electronics Society, Dallas, TX, USA, October 29-November 1, 2014, pp. 2089-2095.
[8] Kaplani, E., Kaplanis, S., Thermal modelling and experimental assessment of the dependence of PV module temperature on wind velocity and direction, module orientation and inclination,*Solar Energy*, 107(2014), pp. 443-460
[9] Perović, B. D., *et al.*, Modeling the effect of the inclination angle on natural convection from a flat plate: the case of a photovoltaic module, *Thermal Science*, 21(2017), 2, pp. 925-938
[10] Fuentes M. K., A simplified thermal model for flat-plate photovoltaic arrays, Sandia Report SAND85-0330, Unlimited Release, Sandia National Laboratories, USA, 1987
[11] Palyvos, J. A., A survey of wind convection coefficient correlations for building envelope energy systems' modeling,*Applied Thermal Engineering*, 28(2008), 8-9, pp. 801-808
[12] Perović, B. D., Modelling the effect of the inclination angle on the efficiency of photovoltaic modules using empirical correlations, Ph.D. thesis, University of Priština in Kosovska Mitrovica, 2018, https://pr.ac.rs/wp-content/uploads/2018/01/bojan_perovic_dd.pdf
[13] Sam, R. G., *et al.*, An experimental study of flow over a rectangular body,*Journal of Fluids Engineering*, 101(1979), 4, pp. 443-448
[14] Holman, J. P., *Heat transfer*, 8th edition, McGraw-Hill, New York, USA, 1997
[15] Kendoush, A. A.,Theoretical analysis of heat and mass transfer to fluids flowing across a flat plate, *International Journal of Thermal Sciences*, 48(2009), 1, pp. 188-194
[16] Churchill, S. W., A comprehensive correlating equation for forced convection from flat plates, *AIChE Journal*, 22(1976), 2, pp. 264-268
[17] Vasant, P. M.,*Meta-heuristics optimization algorithms in engineering, business, economics, and finance*, Information Science Reference, an imprint of IGI Global, Hershey, PA, USA, 2013

[18] Onur, N., Forced convection heat transfer from a flat-plate model collector on roof of a model house,*Heat and Mass Transfer*, 28(1993), 3, pp. 141-145
[19] Turgut, O., Onur, N.,Three dimensional numerical and experimental study of forced convection heat transfer on solar collector surface,*International Communications in Heat and Mass Transfer*, 36(2009), 3, pp. 274-279
[20] Kind, R. J., *et al.*, Convective heat losses from flat-plate solar collectors in turbulent winds,*Journal of Solar Energy Engineering*, 105(1983), 1, pp. 80-85
[21] Sparrow, E. M., *et al.*, Effect of finite width on heat transfer and fluid flow about an inclined rectangular plate, *Journal of Heat Transfer*, 101(1979), 2, pp. 199-204
[22] Shakerin, S.,Wind-related heat transfer coefficient for flat-plate solar collectors, *Journal of Solar Energy Engineering*, 109(1987), 2, pp. 108-110
[23] Francey, J. L., Papaioannou, J.,Wind-related heat losses of a flat-plate collector,*Solar Energy*, 35(1985), 1, pp. 15-19
[24] Motwani, D. G., *et al.*, Heat transfer from rectangular plates inclined at different angles of attack and yaw to an air stream, *Journal of Heat Transfer*,107(1985), 2, pp. 307-312
[25] Jayamaha, S. E. G., *et al.*, Measurement of the heat transfer coefficient for walls, *Building and Environment*, 31(1996), 5, pp. 399-407
[26] Sartori, E.,Convection coefficient equations for forced air flow over flat surfaces, *Solar Energy*, 80(2006), 9, pp. 1063–1071
[27] Incropera, F. P., *et al.*, *Fundamentals of heat and mass transfer*, 6th edition, John Wiley & Sons Inc., New Jersey, USA, 2007
[28] Nižetić, S., *et al.*, Experimental and numerical investigation of a backside convective cooling mechanism on photovoltaic panels, *Energy*, 111(2016), pp. 211-225
[29] Kouadri Boudjelthia, E. A., *et al.*, Role of the wind speed in the evolution of the temperature of the PV module: Comparison of prediction models, *Revue des Energies Renouvelables*, 19(2016), 1, pp. 119-126
[30] Palacio Vega, M. A., *et al.*, Estimation of the surface temperature of a photovoltaic panel through a radiation-natural convection heat transfer model in MATLAB Simulink,Proceedings of the ASME 2016 International Mechanical Engineering Congress and Exposition – IMECE2016, Phoenix, AZ, USA, November 11-17, 2016, pp. 1-8